

zation with concentrated hydrochloric acid. The precipitate washed with water and dried at 75 °C for 24 h gave 3-(chloromercurio)-5-nitrosalicylaldehyde (1.55 g) in 42% yield based on 5-nitrosalicylaldehyde, mp 252 °C dec, uncorrected. Anal. Calcd for C<sub>7</sub>H<sub>4</sub>ClHgNO<sub>4</sub>: C, 20.89; H, 1.00; Cl, 8.82; Hg, 49.89; N, 3.48. Found: C, 20.98; H, 1.00; Cl, 8.49, 8.58; Hg, 50.06; N, 3.44. Although the chloro- and acetoxymurcurio forms are probably equivalent for most applications, we have found that the latter is easily purified whereas the former tends to lose chlorine and form higher melting products on attempted recrystallization. However, if the latter is purified first as illustrated here then the initially isolated chloromercury product is quite suitable for use. The open ring position activated by the ortho hydroxyl is suggested to be the site of mercuration as this position is also meta to both the nitro and aldehyde meta-directing substituents. Mercuration in this position is further indirectly supported by the magnitude of the phenolic pK shift of the mercurial-EDTA complex (cf. Table I and ref 11).

Table I summarizes spectroscopic data, pK<sub>a</sub>, and melting points for 5-nitrosalicylaldehyde and the two mercurials as well as two model compounds formed and examined in situ after reduction of the mercurials with sodium borohydride alone or in the presence of (α-acetyllysyl)aminomethane. The latter was formed after reduction in the presence of a large excess of amine and separated from traces of the benzyl alcohol analogue product by extraction of the latter from acidified solutions of the products. Also included in Table I are two products formed from the borohydride reduction of Schiff's bases derived from the interaction of the 3-(chloromercurio)-5-nitrosalicylaldehyde and the principal curarimimetic neurotoxin<sup>6</sup> from the venom of the Thailand cobra, *Naja naja siamensis*. Figure 2 shows the results of the titration of a freshly prepared solution of mercaptoethanol (13 nM) with 3-(acetoxymurcurio)-5-nitrosalicylaldehyde using the mercurial indicator dye pyridine-2-azo-4'-(N',N'-dimethylaniline) to detect excess mercurial.<sup>5</sup>

The pK<sub>a</sub> of 3-(acetoxymurcurio)-5-nitrosalicylaldehyde is, as expected, similar to that of the 3-(chloromercurio) derivative and to 5-nitrosalicylaldehyde. The relatively large pK<sub>a</sub> differences between the ortho hydroxymethyl- and the (alkylamino)-methyl-substituted phenols may be associated with the ionic and hydrogen-bonded stabilization of the phenolic anion by the protonated amine as well as the inductive withdrawing potential of aminomethylammonium (cf. hydroxymethyl). Different microenvironmental effects on the aminomethyl function modified in the neurotoxin evidently lead to the pK<sub>a</sub> differences observed in derivatives A and B.<sup>7,8</sup>

We used 3-(chloromercurio)-5-nitrosalicylaldehyde to reductively alkylate amino functions of the principal curarimimetic neurotoxin from the venom of the Thailand cobra, *Naja naja siamensis*. Purification of this protein, which bears no free sulfhydryls, from the lyophilized venom (obtained from the Miami Serpentarium) was carried out by the method of Karlsson et al.<sup>9</sup> The protein (0.72 μM) was incubated with 3-(chloromercurio)-5-nitrosalicylaldehyde (2.0 μM) in sodium phosphate (pH 9) and the Schiff's base adducts reduced with sodium borohydride (40 μM). The solution was acidified (pH 5), exhaustively dialyzed against distilled water, and lyophilized. The product was taken up in phosphate buffer (20 mM, pH 4.80) and chromatographed on phosphocellulose using a concave gradient from 0.02 to 1.0 M phosphate (pH 4.80). Three protein peaks were observed, two of which (A and B) possessed the spectrum of the reduced mercurial reagent. These two fractions were radiolabeled upon reduction with sodium [<sup>3</sup>H]borohydride. Their specific activities were approximately equal. The third peak eluted at an ionic strength similar to that observed for the native toxin when chromatographed alone.

While fractions A and B had virtually indistinguishable spectra characteristic of the introduction of 1 mol of reagent per mol of protein, the phenolic pK<sub>a</sub>'s were depressed to differing extents, cf. the model lysylaminomethane adduct. As the crystal structure

of this neurotoxin has been determined,<sup>10</sup> it will be of certain interest to survey the microenvironment of each of the residues modified in light of these pK<sub>a</sub> depressions. However, variation in the pK<sub>a</sub> of nitrophenols introduced into protein is not unexpected. McMurray and Trentham<sup>11</sup> synthesized several mercurial nitrophenols which they used for the modification of protein sulfhydryl groups. They showed that these reagents were sensitive probes of the microenvironment of the thiol group.

Furthermore, though not demonstrated here, there may be additional instances in which the reagents reported may find use in protein crystallographic studies. Isomorphous, heavy-metal derivatives are required to solve the phase problem.<sup>12</sup> The ease of formation of derivatives for the curarimimetic toxins suggests that crystals of other proteins formed or stable at neutral to basic pH may interact directly with the reagents to form heavy-metal derivatives without the need to form a stable linkage via borohydride reduction. The Schiff's base reaction, while kinetically favored at higher pH, may be carried out at or near neutral pH. This reaction will be especially favorable for proteins that contain uniquely reactive amino groups. Normally, proteins that do not possess a sulfhydryl are modified so that one may be introduced. One of several heterobifunctional reagents may be employed.<sup>13-16</sup> The introduced sulfhydryl is then reacted with organomercurials. The class of reagents reported here offers the opportunity to bypass the intermediate step.

Finally, in preliminary experiments we have shown that the two prepared mercurial toxin derivatives retain reactive mercurials capable of mediating the cross-linking of the toxin into sulfhydryl functions in its biological target, the nicotinic acetylcholine receptor.<sup>17-19</sup> Thus, the reagents that are presented here will, we believe, be useful in probing protein-protein interactions.

(12) Green, D. W.; Ingram, V. M.; Perutz, M. F. *Proc. R. Soc. London, Ser. A* **1954**, 225, 287-307.

(13) Benesch, R.; Benesch, R. E. *J. Am. Chem. Soc.* **1956**, 78, 1597-1599.

(14) Benesch, R.; Benesch, R. E. *Proc. Natl. Acad. Sci. U.S.A.* **1958**, 44, 848-853.

(15) Leonis, J. C. R. *Trav. Lab. Carlsberg, Ser. Chim.* **1948**, 26, 315-355.

(16) Mohrbray, S.; Petsko, G. A. *J. Biol. Chem.* **1983**, 258, 5634-5637.

(17) Maelicke, A. *Angew. Chem. Int. Ed. Engl.* **1984**, 23, 195-221.

(18) Karlin, A. *Neurosci. Comment.* **1983**, 1, 111-122.

(19) Cafmeyer, N.; Kelly, R.; Wohlfeil, E.; Hudson, R. A. *Fed. Am. Soc. Expl. Biol.* **1984**, 43, 759.

### The Planar C··C Ring-Opened Form of the Ethylene Oxide Radical Cation. ESR Evidence from Anisotropic <sup>13</sup>C Studies

Xue-Zhi Qin, Larry D. Snow, and Ffrancon Williams\*

Department of Chemistry, University of Tennessee  
Knoxville, Tennessee 37996-1600

Received December 26, 1984

The nature of the ethylene oxide radical cation has recently attracted considerable interest,<sup>1-7</sup> but the experimental studies using solid-state ESR spectroscopy have led to conflicting interpretations<sup>1,2,7</sup> of the hyperfine data. Essentially, the <sup>1</sup>H hy-

(1) Snow, L. D.; Wang, J. T.; Williams, F. *Chem. Phys. Lett.* **1983**, 100, 193.

(2) Symons, M. C. R.; Wren, B. W. *Tetrahedron Lett.* **1983**, 2315; *J. Chem. Soc., Perkin Trans. 2*, **1984**, 511.

(3) Feller, D.; Davidson, E. R.; Borden, W. T. *J. Am. Chem. Soc.* **1983**, 105, 3347; **1984**, 106, 2513.

(4) Bouma, W. J.; Poppinger, D.; Saebø, S.; MacLeod, J. K.; Radom, L. *Chem. Phys. Lett.* **1984**, 104, 198 and references therein.

(5) Clark, T. *J. Chem. Soc., Chem. Commun.* **1984**, 666.

(6) Bally, T.; Nitsche, S.; Haselbach, E. *Helv. Chim. Acta* **1984**, 67, 86.

(7) Ushida, K.; Shida, T., cited as private communication in ref 4.

(11) McMurray, C. H.; Trentham, D. *Biochem. J.* **1969**, 115, 913-921.

**Table I.** ESR Parameters for the Ring-Opened  $^2A_2$  Radical Cations from Ethylene Oxide in  $CFCl_3$ 

radical cation	nucleus	hyperfine couplings/G					spin density	
		$A_x^a$	$A_y^a$	$A_z^a$	$A_{iso}$	$2B^b$	$\rho_{2p_z}^c$	$g_{iso}$
$CH_2OCH_2^+$	$^1H$	15.2	17.2	16.2	16.2			2.0024
	$^{35}Cl$	2.4	2.4	3.2	2.7			
	$^{37}Cl$	2.0	2.0	2.7	2.2			
$^{13}CH_2O^{13}CH_2^+$	$^{13}C$	9.0	9.0	57.2	25.1	32.1	0.42 <sup>d</sup>	2.0024
							0.50 <sup>e</sup>	
	$^1H$	15.2	17.2	16.2	16.2			
	$^{35}Cl$	2.4	2.4	3.2	2.7			
	$^{37}Cl$	2.0	2.0	2.7	2.2			

<sup>a</sup>The z axis is perpendicular to the molecular plane of structure **1** and the x and y axes are arbitrarily directed in this plane.<sup>14</sup> <sup>b</sup>Calculated from  $A_z = A_{iso} + 2B$ . <sup>c</sup> $\rho_{2p_z} = 2B/2B_0$ . <sup>d</sup>Spin population calculated with a  $2B_0$  value of 76.6 G (Morton, J. R.; Preston, K. F. *J. Magn. Reson.* **1978**, *30*, 577) for unit spin population in a  $^{13}C$   $2p_z$  orbital. <sup>e</sup>Using  $2B_0 = 64.5$  G (Morton, J. R.; Rowlands, J. R.; Whiffen, D. H. National Physical Laboratory (U.K.), Rept. No. BPR 13, 1962).

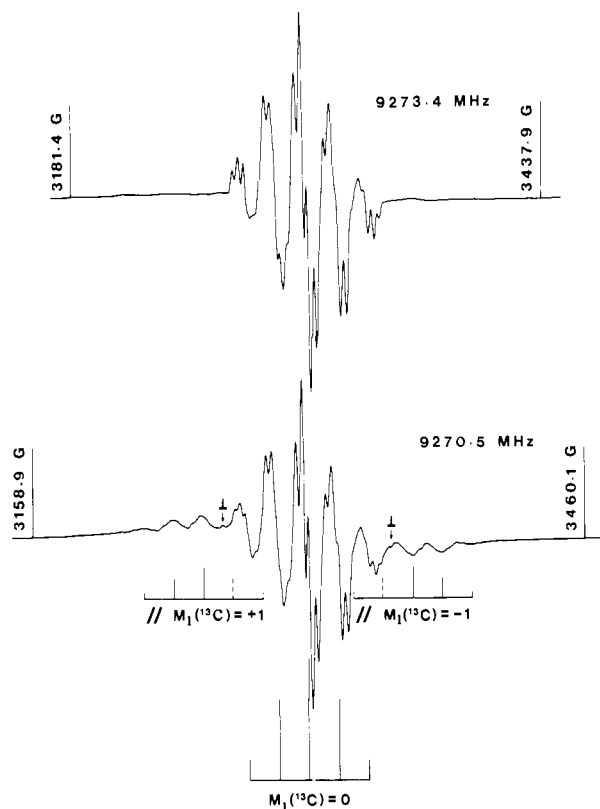
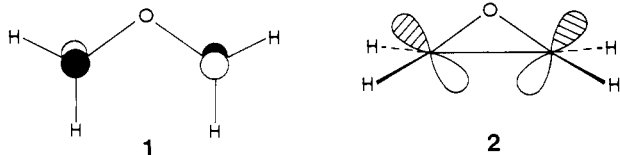


**Figure 1.** First-derivative ESR spectra of the radical cations of unlabeled ethylene oxide (upper) and of [1,2- $^{13}C$ ]ethylene oxide (99%) (lower) in a  $CFCl_3$  matrix at 110 K. The spectra were recorded under identical instrumental conditions after exposure of the  $^{12}C$  and  $^{13}C$  samples to  $\gamma$  radiation at 77 K for doses of 0.7 and 1.4 Mrad, respectively.

perfine splitting ( $A(4H) = 16.2 \pm 0.2$  G) rules out the ring-closed  $^2B_1$  ground state<sup>1,2,8</sup> but does not distinguish between the planar ring-opened  $^2A_2$  state<sup>1</sup> (**1**) and the ring-closed excited  $^2A_1$  state<sup>2</sup> (**2**). However, the ESR spectrum does not show the expected



positive  $g$  shift from free spin for a ring-closed  $^2A_1$  species,<sup>9</sup> and

(8) Kimura, K.; Katsumata, S.; Achiba, Y.; Yamazaki, T.; Iwata, S. "Handbook of He I Photoelectron Spectra of Fundamental Organic Molecules"; Halsted Press: New York, 1981; p 206.

(9) Iwasaki, M.; Toriyama, K.; Nunome, K. *J. Chem. Soc., Chem. Commun.* **1983**, 202. Qin, X.-Z.; Snow, L. D.; Williams, F. *J. Am. Chem. Soc.* **1984**, *106*, 7640.

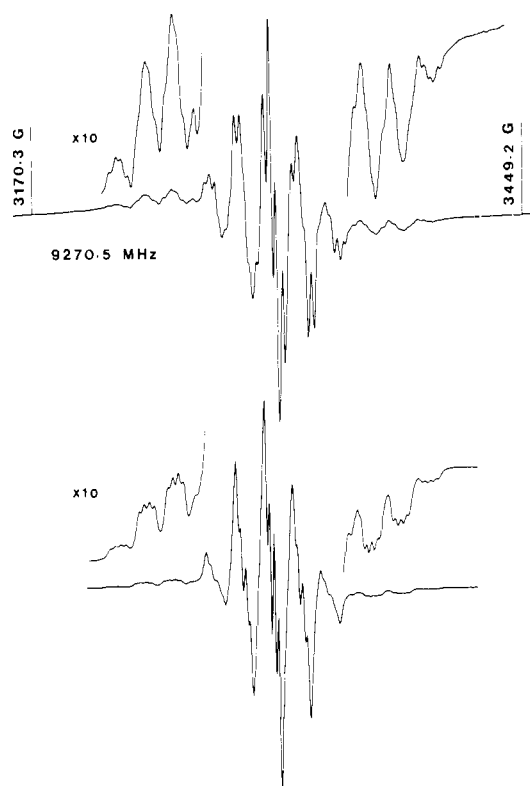


**Figure 2.** Experimental (upper spectrum) and computer-simulated (lower spectrum) first-derivative ESR spectra of the radical cation of 99% [1,2- $^{13}C$ ]ethylene oxide. The experimental spectrum was recorded under the same conditions as in Figure 1 but at a slightly different orientation. The lower spectrum was simulated using the ESR parameters in Table I and a line width of 2.0 G.

high-level theoretical calculations predict that structure **1** lies about 20 kcal mol<sup>-1</sup> below its ring-closed isomers.<sup>4,5</sup>

We have resolved this problem by carrying out ESR studies on 1,2- $^{13}C_2$  (99%) labeled ethylene oxide (Cambridge Isotope Laboratories, Inc.), the cation being generated radiolytically as before<sup>1,2</sup> in the  $CFCl_3$  matrix.<sup>10</sup> As shown in Figure 1, the spectrum of the  $^{13}C$ -labeled cation consists of weak outer features together with a strong set of central lines which is almost an exact replica of the 1:4:6:4:1 hyperfine pattern from the unlabeled cation. This striking similarity immediately suggests that the center lines in the spectrum of the labeled species are the sharp  $M_1(^{13}C) = 0$  components of a triplet<sup>11</sup> resulting from interaction with two equivalent  $^{13}C$  nuclei whose anisotropic hyperfine tensors have

(10) Shida, T.; Haselbach, E.; Bally, T. *Acc. Chem. Res.* **1984**, *17*, 180.

(11) The central features in the spectrum of the  $^{13}C$ -labeled species are approximately 0.5 as intense as those observed in the spectrum of the unlabeled species obtained under identical experimental conditions, in agreement with the 1:2:1 overall intensity ratios of the triplet pattern from the  $^{13}C$  hyperfine interaction.

a common principal axis system.<sup>12</sup> Moreover, since the weak outer features show precisely the same 16-G spacing and intensity distribution as the center quintet, and have characteristic line shapes, they can be assigned to the  $M_I(^{13}\text{C}) = +1$  and  $-1$  parallel components, the hyperfine tensors being axially symmetric. The corresponding perpendicular features are obscured by the strong central lines except for the two marked peaks, which are believed to correspond to the extremities of the perpendicular pattern.

A computer simulation of the powder spectrum<sup>13</sup> using the ESR parameters deduced by inspection<sup>14</sup> (Table I) shows a good fit to the experimental spectrum in Figure 2. The only detail that is not faithfully reproduced is the profile of the quartet superhyperfine substructure from the matrix interaction.<sup>1,15</sup> This varied slightly with sample orientation and shows a greater dependence on the  $M_I(^1\text{H})$  value in the experimental spectrum. Nevertheless, this substructure is evident on all the lines and is clearly resolved in the outermost wing features of the parallel pattern, providing further proof that these outer components are related to the strong central quintet.<sup>16</sup>

The stringent requirement that the two  $^{13}\text{C}$  hyperfine tensors have a common principal axis system is met by structure 1 since the carbon  $2p_z$  orbitals possessing most of the spin density are parallel to each other. On the other hand, the carbon  $2p$  orbitals of the SOMO of structure 2 are not parallel, and computer-simulated ESR spectra for this general case did not give strong central features, as expected.<sup>17</sup> The assignment to the  $^2A_2$  state is also consistent with the magnitude of the spin populations in the carbon  $2p_z$  orbitals as calculated from the  $^{13}\text{C}$  hyperfine anisotropy (Table I). These results show that almost all the spin density resides in these two atomic orbitals, in agreement with structure 1.<sup>18,19</sup>

(12) Cf.: Iwasaki, M.; *Fluorine Chem. Rev.* **1971**, *5*, 1. See pp 14-16 of this review for a comparable example of selective  $^{19}\text{F}$  anisotropic broadening in the powder ESR spectrum of the  $\text{CF}_2\text{CONH}_2$  radical. In the present case, the sharpness of the center lines is accentuated by the nearly isotropic  $g$  tensor.

(13) Kasai, P. H.; McLeod, D., Jr.; McBay, H. C. *J. Am. Chem. Soc.* **1974**, *96*, 6864. Kasai, P. H. *J. Am. Chem. Soc.* **1972**, *94*, 5950.

(14) The  $^1\text{H}$  hyperfine anisotropy is much less than that usually associated with  $\alpha$ -hydrogens in a rigid structure. This is inconsistent with structure 2<sup>9</sup> but can be explained in terms of structure 1 if the exo and endo hydrogens rapidly interchange positions since this would greatly reduce the large anisotropy for field directions in the molecular plane. In view of this dynamical model, the residual  $^1\text{H}$  anisotropy in Table I is not associated with particular directions in the  $xy$  plane.

(15) Analysis of this matrix interaction in  $\text{CFCl}_3$  is complicated by the fact that the precise form of the substructure changes gradually and reversibly with temperature.<sup>1</sup> Although coupling to a single chlorine ( $I = 3/2$ ) nucleus (Table I) seems more consistent with other studies of radical cation-Freon matrix interactions (Snow, L. D.; Williams, F. *Faraday Discuss. Chem. Soc.*, in press) it is, of course, possible that the apparent 1:3:3:1 pattern at 110 K results from coupling to three fortuitously equivalent fluorines, each fluorine ( $I = 1/2$ ) being necessarily in a separate  $\text{CFCl}_3$  molecule.

(16) ESR studies of the doubly  $^{13}\text{C}$ -labeled radical cation in the  $\text{CF}_3\text{CCl}_3$ ,  $\text{CCl}_4$ , and  $\text{SF}_6$  matrices also reveal the presence of an intense central ( $M_I = 0$ ) quintet although the  $M_I = \pm 1$  parallel components are generally not as well resolved as in the  $\text{CFCl}_3$  matrix. In the  $\text{CCl}_4$  matrix at 140 K, the center quintet consists of sharp lines with no substructure giving  $A(4\text{H}) = 16.0$  G and  $g = 2.0024$ , while a tentative analysis of the outer features yields the parameters  $A_1(^{13}\text{C}) = 41.0$  G and  $A_2(^{13}\text{C}) = 17.3$  G. Although these latter values differ from those obtained in  $\text{CFCl}_3$  (Table I) at 110 K, the calculated isotropic values (25.1 (CFCl<sub>3</sub>) and 25.2 G (CCl<sub>4</sub>)) are very similar, suggesting that the reduced  $^{13}\text{C}$  anisotropy in  $\text{CCl}_4$  at 140 K results from greater motional averaging.

(17) Cf.: Shiotani, M.; Nagata, Y.; Sohma, J. *J. Am. Chem. Soc.* **1984**, *106*, 4640.

(18) A referee has informed us that Dr. M. Iwasaki and his co-workers have recently reported the observation of a slightly asymmetric form of the planar ring-opened ethylene oxide radical cation<sup>3,4</sup> in the  $\text{SF}_6$  matrix at 4-30 K (Muto, H.; et al. *Jpn. Radiat. Chem. Symp.* **27th** **1984**, 87), the symmetric structure observed at higher temperatures being attributed to dynamical averaging between the two asymmetric forms.<sup>3,4</sup> We have examined the spectrum of the radical cation in  $\text{CFCl}_3$  down to 4 K and the symmetric or time-averaged  $^2A_2$  structure is retained down to ca. 15 K. Below this temperature the spectrum showed very distinct changes but the pattern is not easily analyzed, possibly on account of complications resulting from the matrix interaction.

(19) In contrast to the symmetric and asymmetric planar forms of the ring-opened ethylene oxide radical cation, we have recently observed that the localized and presumably twisted form of this cation is produced in the  $\text{CFCl}_2\text{CF}_2\text{Cl}$  matrix at 77 K<sup>20</sup> (cf.: Qin, X.-Z.; Williams, F. *Chem. Phys. Lett.* **1984**, *112*, 79. Qin, X.-Z.; Snow, L. D.; Williams, F. *J. Am. Chem. Soc.* **1984**, *106*, 7640).

**Acknowledgment.** We are indebted to Dr. Paul Kasai for kindly providing us with a copy of his computer program for the simulation of powder ESR spectra. This research has been supported by the Division of Chemical Sciences, U. S. Department of Energy (Report No. DOE/ER/02968-157).

(20) Qin, X.-Z.; Snow, L. D.; Williams, F. *J. Phys. Chem.*, submitted for publication.

## Determination of Adsorption Conformation from Surface Resolution Analysis

Dina Farin, Anna Volpert, and David Avnir\*

Department of Organic Chemistry  
The Hebrew University of Jerusalem  
Jerusalem 91904, Israel

Received January 28, 1985

The conformation of an adsorbed molecule on a surface is a key parameter which dictates the interactions, chemical and physical, that the molecule can undergo at the surface. This is so because adsorption, unlike dissolution, exposes specific moieties either outward to incoming reagents or inward to a (catalytic) surface and, because the nonsymmetric "one-sided-solvation" by the surface, distorts ground-state conformations of adsorbates, consequently affecting (photo)chemical reaction pathways.<sup>1</sup>

Despite its importance, conformational aspects of adsorbates are still poorly understood. A first-order approach is based on simple chemical arguments, e.g., that adsorbate/adsorbent relative alignment is determined by the availability of hydrogen bonds. Fine tuning of this picture is done by determining the effective cross-sectional area ( $\sigma$ ) of the adsorbate by one of several methods:<sup>2</sup> (a) By the use of a molecular model and its projections,<sup>3,4</sup> it is possible to provide a rough estimate of  $\sigma$  for rigid molecules, e.g., aromatic polycyclic hydrocarbons. (b)  $\sigma$  can be calculated from liquid density values, assuming sphericity.<sup>2</sup> This assumption limits the method to short or branched molecules. The two methods are further limited to adsorbates for which conformational distortion by adsorption can be neglected. (c) Methods a and b do not provide information on the effective  $\sigma$ , i.e., a value taking into account the envelope of the many conformers of flexible adsorbates and the empty areas, if such exist, between one occupied adsorption site and the next. A common method which tries to overcome this problem indirectly is to divide the surface area from the  $\text{N}_2$ -BET method<sup>5</sup> by the monolayer value of the investigated molecule.<sup>2,6</sup> This procedure is proper only for smooth surfaces, i.e., for surfaces of low fractal dimension, in which the available surface area is independent of probe size. An unfortunate common error is to apply this procedure to highly irregular surfaces for which surface accessibility is strongly dependent on probe size.<sup>1</sup> Furthermore, it is quite unclear whether values determined for smooth surfaces are applicable to wiggly ones.

Here we wish to report on a new approach in conformational analysis of adsorbates, which seems to be free of the above-mentioned disadvantages. It elucidates  $\sigma$  directly from the adsorption experiment and from resolution analysis of the surface. Resolution (fractal) analysis is a rapidly growing tool in many domains of natural sciences, where geometrical irregularity characterizes the investigated system.<sup>7</sup>

(1) E.g.: Bauer, R. K.; Bornstein, R.; De Mayo, P.; Okada, K.; Rafalska, M.; Ware, W. R.; Wu, K. C. *J. Am. Chem. Soc.* **1982**, *104*, 4635.

(2) McClellan, A. L.; Harnsberger, H. F. *J. Colloid Interface Sci.* **1967**, *23*, 577.

(3) Amoores, J. E. *Ann. N. Y. Acad. Sci.* **1964**, *116*, 457.

(4) Scott, R. P. W.; Simpson, C. F. *Faraday Symp. R. Soc. Chem.* **1980**, *15*, 69.

(5) Brunauer, S.; Emmett, P. H.; Teller, E. *J. Am. Chem. Soc.* **1938**, *60*, 309.

(6) E.g.: Nay, M. A.; Morrison, J. L. *Can. J. Res., Sect. B* **1949**, *27*, 205.